Journal of Computational Neuroscience, 2, 117–130 (1995)

Electrical Consequences of Spine Dimensions in a Model of a Cortical Spiny Stellate Cell Completely Reconstructed from Serial Thin Sections

IDAN SEGEV
Department of Neurobiology, Institute of Life Sciences and Center of Neural Computation, Hebrew University, Jerusalem, 91904, Israel

ALON FRIEDMAN
Department of Physiology, Center for Brain Research, Faculty of Health Sciences, Ben-Gurion University of the Negev, Beersheva, Israel

EDWARD L. WHITE
Department of Morphology, Center for Brain Research, Faculty of Health Sciences, Ben-Gurion University of the Negev, Beersheva, Israel

MICHAEL J. GUTNICK
Department of Physiology, Faculty of Health Sciences, Ben-Gurion University of the Negev, Beersheva, Israel
gutnick@bgumail.bgu.ac.il

Received July 15, 1994; Revised December 21, 1994; Accepted December 21, 1994

Action Editor: Charles Wilson

Abstract. We built a passive compartmental model of a cortical spiny stellate cell from the barrel cortex of the mouse that had been reconstructed in its entirety from electron microscopic analysis of serial thin sections (White and Rock, 1980). Morphological data included dimensions of soma and all five dendrites, neck lengths and head diameters of all 380 spines (a uniform neck diameter of 0.1 μm was assumed), locations of all symmetrical and asymmetrical (axo-spinous) synapses, and locations of all 43 thalamocortical (TC) synapses (as identified from the consequences of a prior thalamic lesion). In the model, unitary excitatory synaptic inputs had a peak conductance change of 0.5 nS at 0.2 msec; conclusions were robust over a wide range of assumed passive-membrane parameters. When recorded at the soma, all unitary EPSPs, which were initiated at the spine heads, were relatively iso-efficient; each produced about 1 mV somatic depolarization regardless of spine location or geometry. However, in the spine heads there was a twentyfold variation in EPSP amplitudes, largely reflecting the variation in spine neck lengths. Synchronous activation of the TC synapses produced a somatic depolarization probably sufficient to fire the neuron; doubling or halving the TC spine neck diameters had only minimal effect on the amplitude of the composite TC-EPSP. As have others, we also conclude that from a somato-centric viewpoint, changes in spine geometry would have relatively little direct influence on amplitudes of EPSPs recorded at the soma, especially for a distributed, synchronously activated input such as the TC pathway. However, consideration of the detailed morphology of an entire neuron indicates that, from a dendro-centric point of view, changes in spine dimension can have a very significant electrical impact on local processing near the sites of input.

Keywords: compartmental model, dendritic spines, electron microscopy, barrel cortex, mouse, thalamo-cortical, asymmetrical synapses

Introduction

It has been suggested that spine dimensions, in particular those of the spine neck, may play a key role in determining the effectiveness of synapses that contact the spine head membrane. By this hypothesis, the spine neck operates as a variable resistor that controls the amount of current that a synapse produces at the spine head (Rall, 1974; Rinzel, 1982; Crick, 1982; Koch and Poggio, 1983; Wilson, 1984; Brown et al., 1988; Segev and Rall, 1988; and see review in Koch and Zador, 1993). Originally, this hypothesis was based on the assumption that spine membrane is passive and that input onto the spine head is sufficiently powerful to

operate in its nonlinear range (close to the synaptic reversal potential). This situation would arise if the synaptic conductance were large relative to the input conductance at the spine head. In this voltage regime, the amount of current generated by the synaptic input (and thus the amount of charge that reaches the soma) can be controlled by the value of the spine neck resistance, which is directly proportional to the length of the spine neck and inversely proportional to the square of its diameter. However, several authors have pointed out that if the excitatory synaptic conductance at the spine head is small (<1.0 nS), as suggested by recent patch-in-slice experiments (Stern et al., 1992), spines will operate in a voltage range far from saturation, and changes in neck diameter will therefore not affect the amount of synaptic current reaching the soma (Turner, 1984; Kawato and Tsukahara, 1984; Koch and Zador, 1993). Here, we consider an actual neuron and all of its spines and synapses in an attempt to assess the relative electrical importance of spine dimension.

The dimensions of dendritic spines cannot be precisely determined with the light microscope. Thus, the morphological information required to understand how synaptic inputs are processed by spiny neurons (the majority of cells in the cortex) can be obtained only from an electron microscope study. Furthermore, only the electron microscope can provide critical information as to synaptic type (symmetrical versus asymmetrical), as well as the details of synaptic size and exact location. Such information for a spiny neocortical neuron has been obtained in its entirety for only one cell: a spiny stellate neuron in the somatosensory cortex of the mouse, that was fully reconstructed from serial thin sections (White and Rock, 1980). The quantitative information available about the morphology and innervation of this cell is unprecedented. The dimensions of the five dendrites and 380 spines and the sites and types of all synapses that contact the soma-dendritic surface are known. In addition, a degeneration experiment enabled identification of all the 43 thalamocortical (TC) synapses contacting the cell. Thus, this neuron offers a unique opportunity to utilize a modelling study as a tool to understand the functional significance of the details of neuronal morphology and synaptic architecture in the cortex. Specifically, it allows one to examine how variability in spine neck dimensions and spine location would be reflected as variability in the somatic EPSP. One can also examine the effect of changing the dimensions of spines receiving the TC input, thereby exploring whether such changes are likely to play a role in plastic modulation of the thalamocortical interaction.

Compartmental modeling techniques provide a general theoretical framework for synthesis of the detailed morphology of a reconstructed cell with its electrical properties (Rall, 1964; see review by Segev et al., 1989). Here, we utilize compartmental modeling for the analysis of the passive behavior of the cell. Because electrophysiological measurements were not made from the reconstructed spiny stellate cell, we rely on estimates based on the literature for values of biophysical parameters of the membrane and cytoplasm and for characteristics of the synaptic input. Nevertheless, we are able to offer relatively robust answers to questions concerning the functional significance of spine dimensions. Our computations suggest that even with a purely passive dendritic membrane, because of significant variability in spine dimensions, some distal excitatory inputs on spines may be as efficient as proximal spiny inputs in contributing to somatic depolarization. Also, in general, for inputs that involve activation of many synapses, as in TC activation, changing spine neck dimensions is not likely to be an important electrical mechanism for determining the efficacy of such inputs. However, changes in spine dimension can have a very significant *electrical* impact on local processing at the postsynaptic sites. Preliminary results of this study have appeared in abstract form (Segev et al., 1989).

Methods

Morphology

The morphological characteristics of the cell were previously described in detail (White and Rock, 1980). Briefly, the ventrobasal nucleus in a two-month-old male CD/1 mouse was lesioned electrolytically using an approach that avoided damage to nuclei or pathways other than those linking the thalamus directly with the primary somatosensory cortex. Cortex was impregnated by the Golgi method, gold-toned, stained with uranyl acetate, and embedded in plastic. The layer IV spiny stellate neuron described here (Figure 1A) was sectioned into about 350 serial thin sections that were mounted onto slotted grids. Approximately 5,000 electron micrographs, printed at a final magnification of 20,000×, were made of each labeled profile on each thin section of the series. The locations of all asymmetrical (including degenerating thalamocortical) synapses and symmetrical synapses were marked on the prints; these were then used to

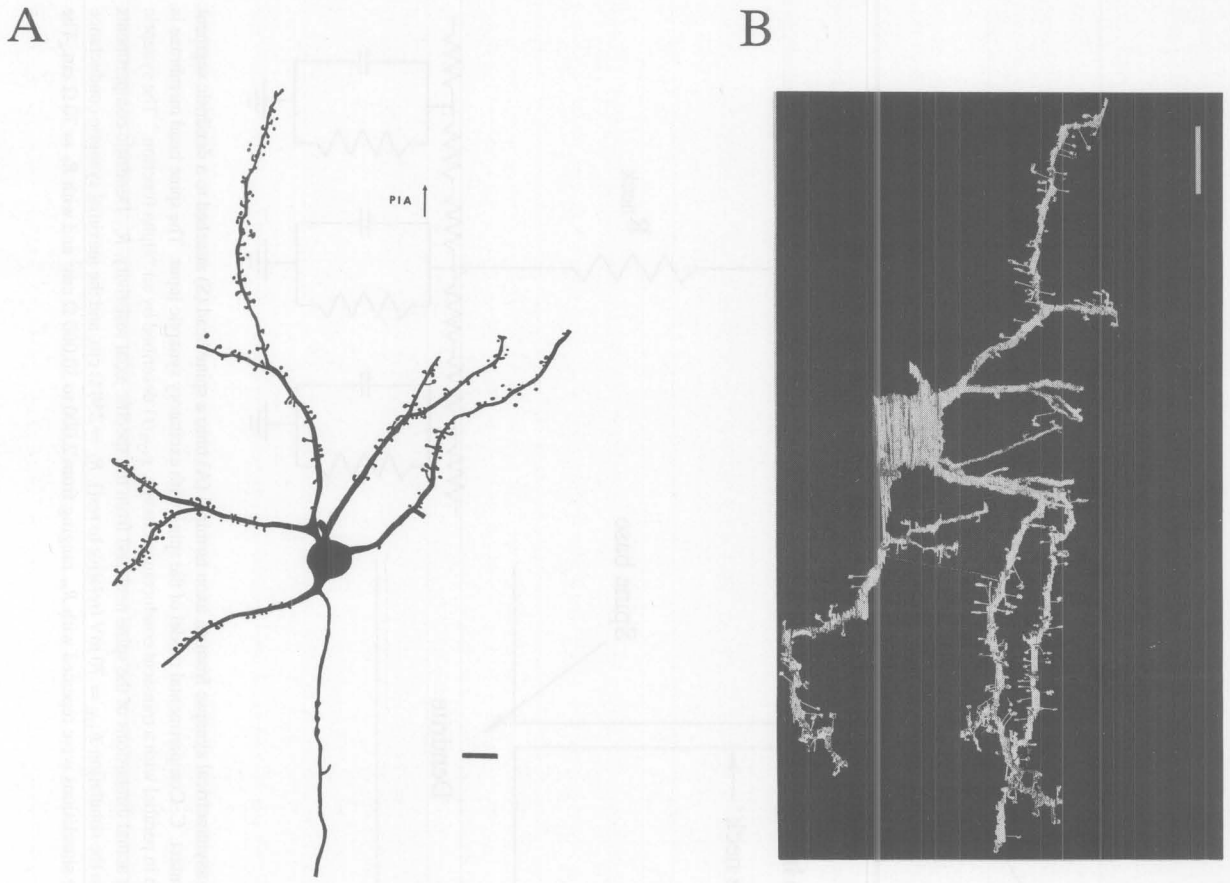

Figure 1. A. Drawing of montage of light micrographs taken at 20 planes of focus, showing a Golgi impregnated/deimpregnated spiny stellate cell from layer IV of mouse primary somatosensory (barrel) cortex. Note that this neuron has five spiny dendrites and one axon coursing toward the white matter. B. Photograph of a wooden model of this spiny stellate cell, which was reconstructed in three dimensions from electron micrographs of 350 serial thin sections. Scale bars: 10 μm.

reconstruct the neuron from wooden slabs of appropriate thickness using the best-fit alignment of structures in adjacent sections (Figure 1B). The result was a three-dimensional representation of the spiny stellate cell and its synaptic inputs from which accurate measurements were obtained by placing a ruler directly on the reconstruction. Because it was not always possible to accurately reconstruct and measure the diameter of the spine necks, we estimated all spine neck diameters to be 0.1 μm (Benshalom, 1989).

Compartmental Model

The anatomical data served as a basis for constructing a detailed compartmental model of the cell. A full account on the theoretical basis for the compartmental modeling approach can be found in Rall (1964) and Segev et al. (1985; 1989). Briefly, the membrane of each dendritic segment is lumped into a passive, isopotential, *R-C* element; this membrane compartment is connected to neighboring membrane compartments via axial resistances representing the cytoplasmic resistivity of the dendrite. A total of 83 compartments were required to represent the five dendrites and the soma of the reconstructed cell without spines. Three hundred eighty dendritic spines were identified in this cell; the head dimensions and neck length of each of these spines were measured. An EM picture of one spine receiving an asymmetrical input at its head is shown in Figure 2A. For the model, spines were represented by spine head membrane connected to the dendrite via a cylindrical spine neck (Figure 2B). The spine head membrane was modeled by an isopotential *R-C* compartment, the values for *R* and *C* were calculated from

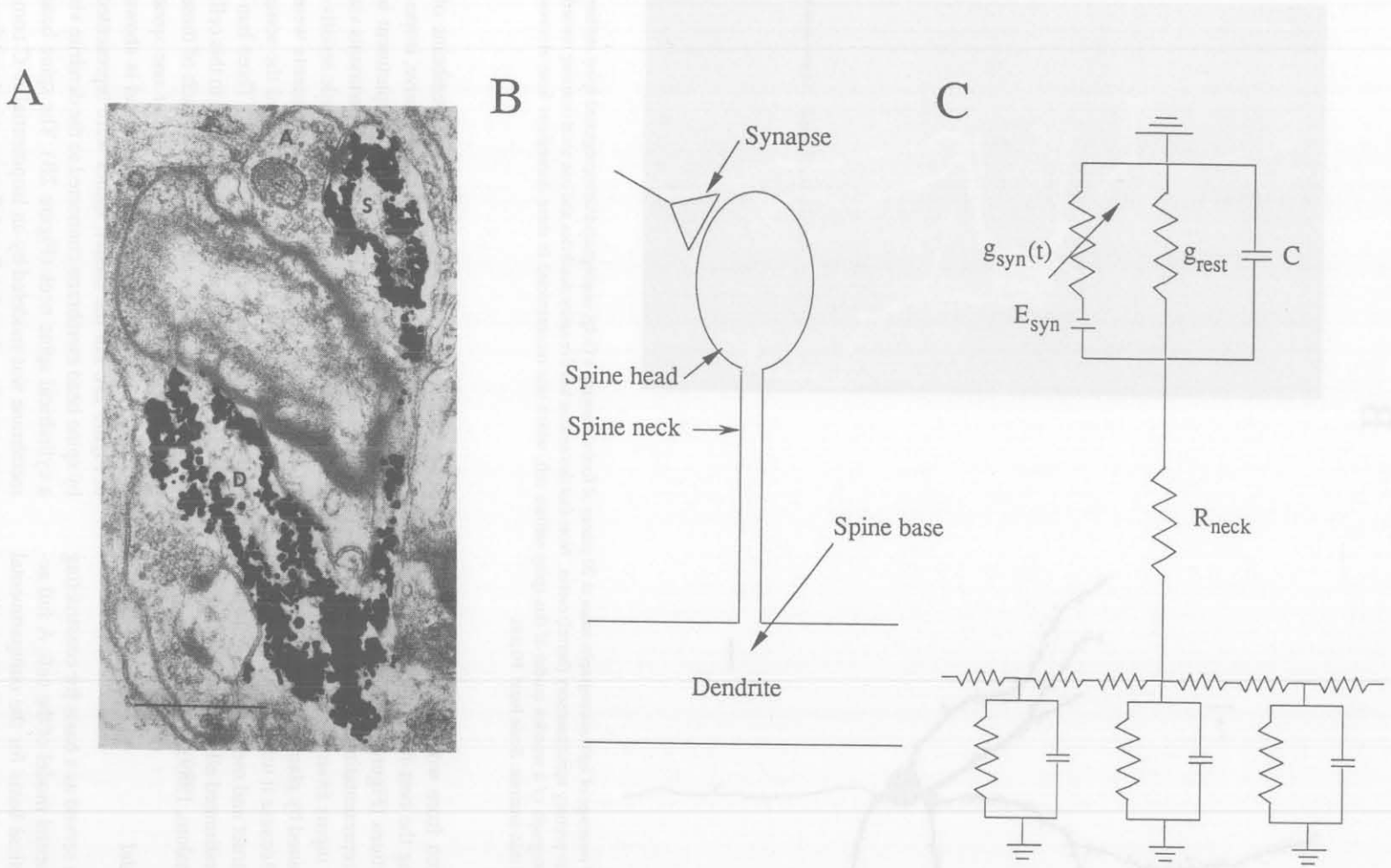

Figure 2. From spine morphology to spine model. A. Electron micrograph of an asymmetrical synapse from an axon terminal (A) onto a spine head (S) attached to a dendritic segment (D). Scale bar: 0.5 μm. B. Schematic representation of the spine with a synaptic contact. C. Compartmental model of the spine with excitatory synaptic input. The spine head membrane is represented by the resting conductance, g_{rest}, in parallel with a capacitance, C; both in parallel with a transient conductance change, $g_{syn}(t)$ described by an "alpha function." The synaptic battery is denoted by E_{syn}. The spine neck resistance (R_{neck}) is calculated from the actual dimensions of the spine neck and from the specific axial resistivity, R_i. Dendritic compartments are modeled as passive R-C elements, connected to each other by axial resistance. In the simulation $E_{syn} = 70$ mV (relative to rest), $R_i = 250\ \Omega$ cm, and the maximal synaptic conductance is 0.5 nS at 0.2 msec. Specific membrane resistance was 8,000 Ω cm^2; some of the simulations were repeated with R_m ranging from 2,000 to 50,000 Ω cm^2 and with $R_i = 70\ \Omega$ cm. The specific membrane capacitance was 1 μF/cm^2.

the actual head area and the values chosen for R_m and C_m. This compartment was connected to the spine base by a single resistance (R_{neck}) representing the spine neck resistance (Figure 2C). The value for R_{neck} was calculated from the actual length of the spine, an assumed diameter of 0.1 μm (Benshalom, 1989) and the value chosen for R_i. Values ranged from 27 to 540 MΩ.

In dendritic spines that receive an asymmetrical (excitatory) synaptic input, an additional conductive branch was added in parallel to the R-C elements. This consisted of a time-varying conductance change (g_{syn}) in the form of an "alpha" function (proportional to $g_{max}(t/t_p)e^{(1-t/t_p)}$, where g_{max} is the amplitude of the conductance change obtained at $t = t_p$). This transient conductance change was connected in series to the synaptic battery (E_{syn}) (Figure 2C; see also Segev and Rall, 1988). Based on experimentally determined characteristics of cortical glutamatergic synapsis of the AMPA type (Stern et al., 1992), asymmetrical synaptic inputs were modeled by a brief conductance change with g_{max} of 0.5 nS and $t_p = 0.2$ msec, and a depolarizing battery of 70 mV relative to the resting potential (denoted here as zero). In the present study, C_m was set at its generally accepted value of 1 μF/cm^2. The standard value for R_m was set at 8,000 Ωcm^2 along the soma-dendritic (and spine) surface (that is, the membrane time constant, τ_m, is 8 msec), and R_i was 210 Ωcm. However, to examine the robustness of our results, most of the computations were repeated with R_m ranging from 2,000 to 32,000 Ωcm^2 and with R_i of 70 Ωcm.

The dendrogram in Figure 3 plots the five dendrites of the modeled neuron. Dendritic spines receiving thalamocortical input are marked by filled circles at their corresponding dendritic location. Note that the dendrites were relatively short and thin and that they showed a small degree of branching. The total dendritic length was 680 μm. The division of this dendogram into 83 segments (each represented by a single compartment) yielded an average segment length of 0.03λ (with $R_m = 8{,}000$ Ωcm^2 and $R_i = 210$ Ωcm). This is much shorter than the refinement needed for convergence of the discrete (compartmental) model to the continuous (cable) model (Segev et al., 1985). The input resistance of the modeled cell was 540 MΩ (660 MΩ without dendritic spines). The transient response of the model to synaptic inputs was simulated initially using SPICE (Segev et al., 1985, 1989) and later using NEURON (Hines, 1989). In all computations, a temporal integration step (Δt) of 20 μs was used.

Results

The morphology and synaptic connections of the neuron examined were typical for spiny stellate cells in mouse barrel cortex (White, 1989). Specifically, the cell body, approximately 10 μm in diameter, received 49 symmetrical synapses, one asymmetrical synapse, and four that were difficult to characterize. The five primary dendrites extending from the cell body and their branches received 68 symmetrical synapses onto their shafts and 373 synapses onto their spines, of which 359 were asymmetrical and 14 symmetrical. Most spines received only one asymmetrical synapse; in eight instances a spine received both a symmetrical and an asymmetrical synapse. In many instances, it was not possible to determine accurately the diameters of spine necks, but a survey of the original material indicated that the narrowest diameter of spine necks was approximately 0.1 μm. A similar value has been reported for the narrowest diameters of spine neck in an extensive analysis of the morphological parameters of dendritic spines belonging to mouse spiny stellate cells (Benshalom, 1989). In that study, no consistent relationship was observed between the diameters of spine necks and their lengths, the sizes of their heads, or the distance of the spine from the cell body.

The distribution of the spine-neck lengths along dendrite 5 (top schematic), as a function of distance from soma is depicted in Figure 4. Spines on side branches were not included in this graph. Less than 10% of the total number of spines on this dendrite were situated along the proximal 20 μm. The necks of these spines tend to be shorter than the average. Along the rest of the dendrite, spines were distributed rather uniformly, with neck lengths ranging between 0.15 and 1.6 μm. The distributions of spines in the other four dendrites was qualitatively not different than that illustrated in Figure 4 (not shown). Analysis of the whole population of 380 dendritic spines in this cell yielded an average spine length of 0.89 ± 0.57 μm (mean $\pm$ SD); the range was 0.05 to 2.85 μm. The membrane area of the spine heads was between 0.008 and 8.04 μm^2 (average was 0.7 ± 0.75 μm^2). The average volume of the spine head was 0.07 ± 0.18 μm^3 (the range was 0.000065 to 2.14 μm^3). The total surface area of the cell was 1,900 μm^2, of which the spine necks and heads contributed about 20% (390 μm^2).

Figure 5 shows the unitary EPSPs that were produced by separate activation of three of the TC synapses on dendrite 5; these were located proximally, distally, and midway along the dendrite. For each synapse,

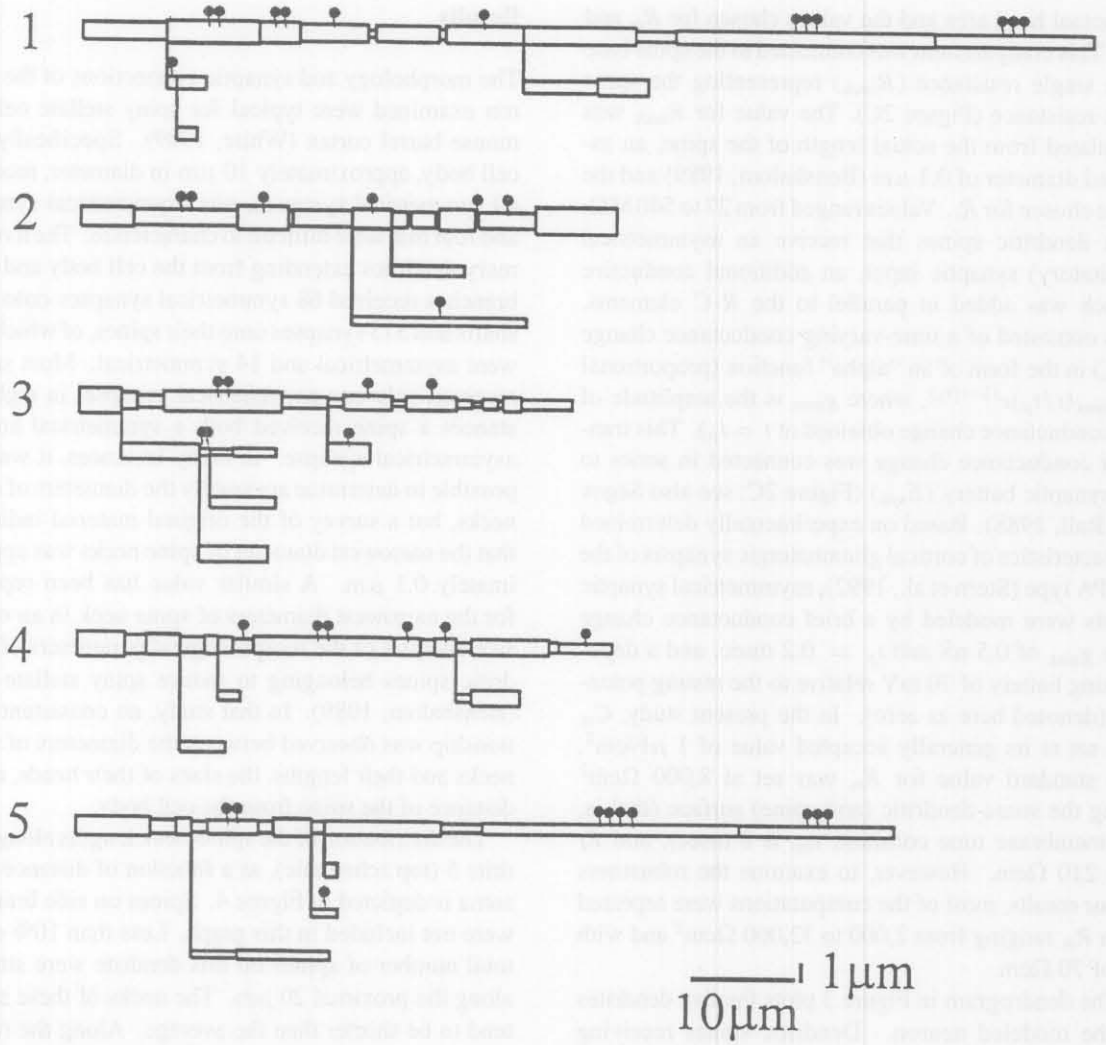

Figure 3. Dendrogram of the modeled spiny stellate neuron. The neuron has five dendrites that were modeled by 82 dendritic compartments (rectangles) and one compartment for the soma (not shown). Filled circles denote thalamocortical synapses (43 total).

the EPSP as recorded at the spine head (top trace), at the spine base (middle trace) and at the soma (lower trace). For the cases chosen, amplitudes at the spine heads and at the soma were nearly identical, whereas the sizes of EPSPs recorded at the bases of these spines were markedly different, reflecting the differences in the input impedance at these locations. This figure demonstrates that for a given set of synaptic parameters, synapses located at different electrical distances from the soma can produce somatic EPSPs of similar amplitude. The somatic EPSP amplitudes were similar in this simulation because these three synapses were located on spines whose neck lengths were such that lower R_{neck} values compensated for the greater attenuation from the more distal spine. Of course, the rise times of the three somatic EPSPs were quite different, being longer for the more distal synapse (Rall, 1967). As illustrated in the graph of Figure 4, there was no systematic, compensatory distribution of spine neck lengths along the dendrites of this cell. Figure 5 does demonstrate, however, that as far as EPSP amplitude is concerned, the morphologies of dendritic spines can cause distal inputs and proximal inputs to be of equivalent efficiency at the soma.

In order to explore the range of somatic EPSP amplitudes expected from the activation of a single spiny synapse, we simulated activation of each of the synapses impinging on the dendritic spines of

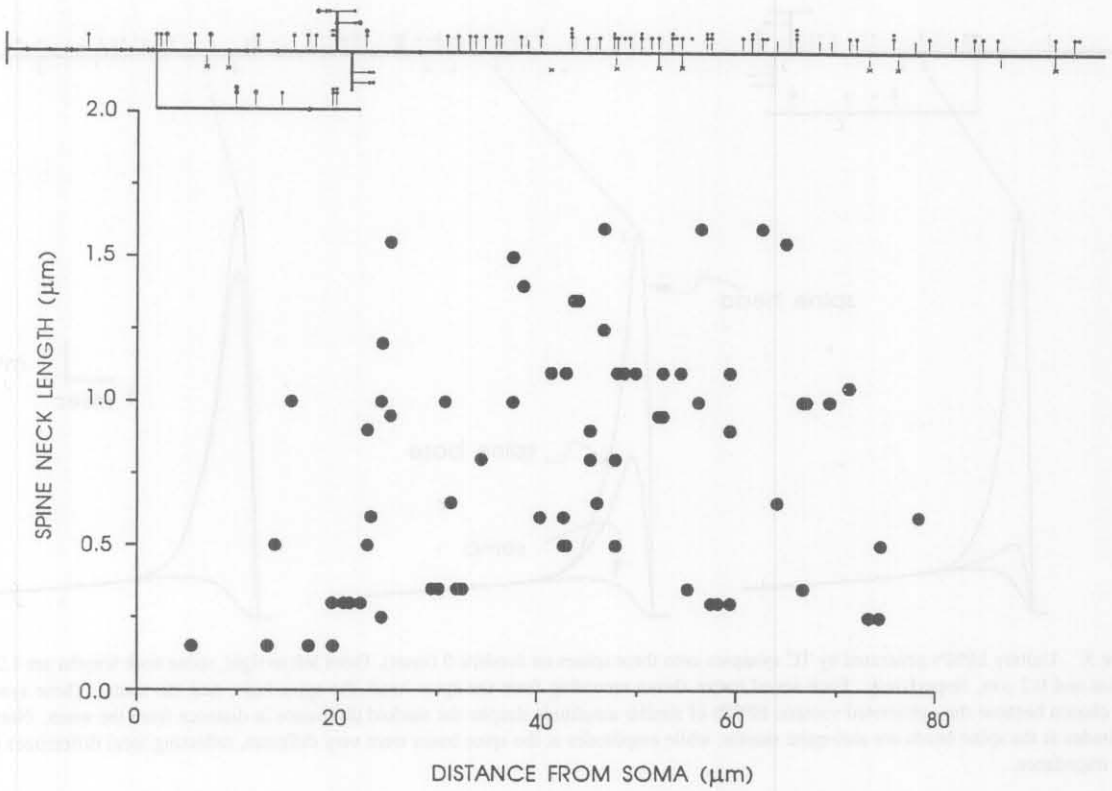

Figure 4. Distribution of spine neck length as a function of distance from soma for dendrite 5. Note the large (20-fold) variability in the spine neck length. Inset at the top shows the relative positions of the spines and synapses (see Figure 12 in White and Rock, 1980). Lines normal to the dendrite axis: spines. Filled circles: asymmetrical synapses. Crosses: TC (asymmetrical) synapses. Bull's eyes: symmetrical synapses. Two symbols at the tip of one line indicates two synapses onto two spines located equidistant from the soma.

dendrite 5, one at a time. The result, including the consequences of activation of spines on the side branches, is illustrated in Figure 6. Although, in the model, each spine connects at one of the 11 compartments simulating this dendritic shaft, the results are plotted as a function of actual distance of each spine base from the soma (filled circles). The effect of cable distance is reflected by the general tendency of the EPSPs to be smaller with increased distance from the soma. In addition, because of variability in spine dimensions, at any given location there is a noticeable (~10%) variability in the EPSP amplitude. For comparison, we constructed a "prototype" spine, whose dimensions were the mean neck length and head diameter of all spines on the cell. This spine was added to each of the compartments and a single excitatory input was activated at its head (triangles). Since identical input parameters were used for each point in this figure, deviation from the prototype values reflects the variability in somatic EPSPs conferred by the variability in spine dimensions. As mentioned above, this variability accounted for the finding that certain distal synapses were more effective than other, more proximal synapses. Note also that for the proximal 20 μm the data points lie above the corresponding prototype values, reflecting the tendency of the proximal spines to have shorter necks than the average.

The variability in the EPSP amplitude at any given location implies that, for the parameters chosen, some spines do not behave as linear current sources. Namely, synapses on spines with long necks generate sufficient local depolarization to decrease synaptic driving force, and thus less synaptic current is produced compared to synapses on spines with shorter necks. Nonetheless, the variability in the somatic recordings (from 1.18 mV to 0.86 mV in Figure 6, 35% change) largely reflects electrotonic distances of the spine bases from the soma, with only a 10% influence of spine dimensions.

In the simulation illustrated in Figure 6, in which R_m was 8,000 Ωcm^2, the range of somatic unitary EPSP

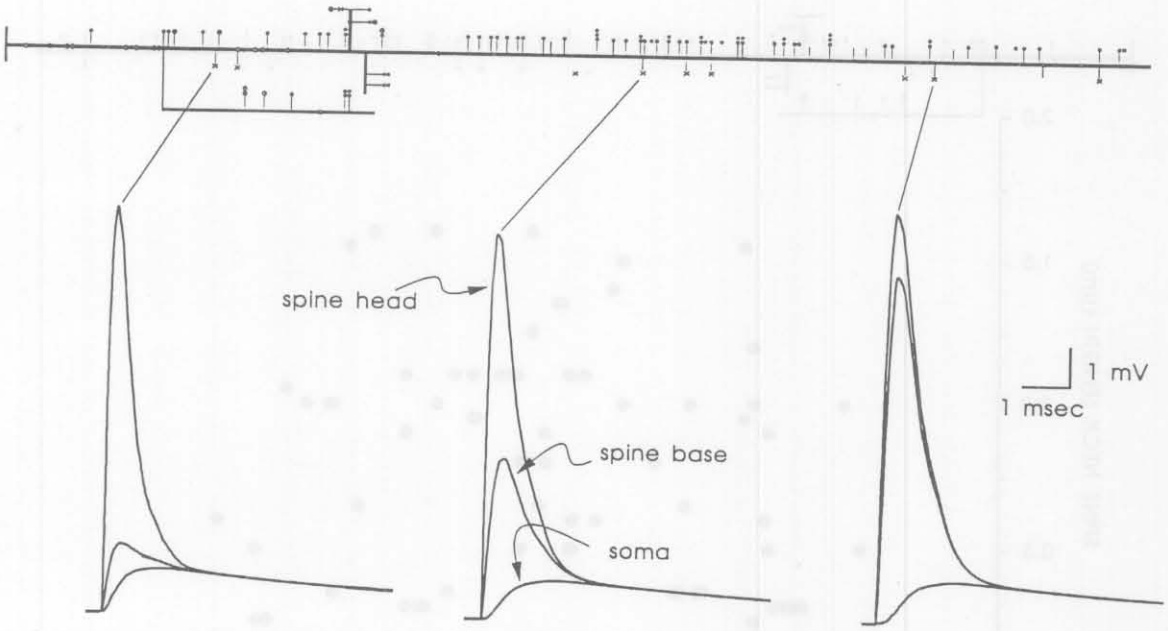

Figure 5. Unitary EPSPs generated by TC synapses onto three spines on dendrite 5 (inset). From left to right, spine neck lengths are 1.2 μm, 0.7 μm and 0.2 μm, respectively. Each set of traces shows recording from the spine head, the spine base, and the soma. These synapses were chosen because they generated somatic EPSPs of similar amplitude despite the marked difference in distance from the soma. Note that amplitudes at the spine heads are also quite similar, while amplitudes at the spine bases were very different, reflecting local differences in the input impedance.

amplitudes was between 0.86 mV and 1.18 mV. In order to test the effect of R_m on this range, we repeated the simulation with R_m values of 2,000 Ωcm^2 and 32,000 Ωcm^2, and obtained ranges of 0.64 to 1.03 mV and 0.97 to 1.23 mV, respectively. Thus, as expected from a brief input, the range was found to be relatively insensitive to a sixteenfold difference in R_m (Nitzan et al., 1990). That individual EPSPs are relatively large is in agreement with recent experimental findings showing that single EPSPs in cortical neurons can be a few mV in size (Thomson, 1993a, 1993b).

Figure 7 displays the results of the same simulation as Figure 6, but in this case the amplitudes of unitary EPSPs at the spine heads (filled squares), the spine bases (filled triangles), and the soma (filled circles) are all plotted at the same scale. An extremely broad distribution of EPSP amplitudes was recorded at the spine heads (from 2 mV to 19 mV), reflecting the large differences in input impedance at the spine head. Comparison of this graph with the distribution of spine neck lengths on this dendrite (Figure 4) reemphasizes the point that the primary source of the difference is variability in spine dimensions. In the model, for spines inserting at the same dendritic compartment, longer necks, and consequently higher R_{neck} are associated with larger EPSPs generated at the spine head. Another source for the variability in the EPSPs at the spine head is the variability in the input impedance at the spine base ($R_{\text{head}} = R_{\text{neck}} + R_{\text{base}}$), which increased as a function of distance from the soma. This explains the tendency of EPSPs on more distally located spines heads to be larger.

This increase in dendritic input impedance with distance from the soma is apparent in the distribution of EPSPs as recorded at the spine base (filled triangles). What is most obvious about recordings in the dendrite is the relative similarity of EPSP amplitudes within any given dendritic compartment. This accounts for the steplike appearance of this curve, reflecting the division of dendrite 5 into discrete compartments in the model.

The most striking feature of Figure 7 is that, whereas the variation in EPSP amplitudes at the spine heads is tenfold, it is only about fivefold at the spine bases, and at the soma (filled circles) it is less than twofold. From a somato-centric viewpoint, all the synapses along this dendrite are essentially iso-efficient, while from a dendro-centric viewpoint, they differ markedly.

We were interested in exploring the effect of thalamocortical (TC) activation on this neuron. The number

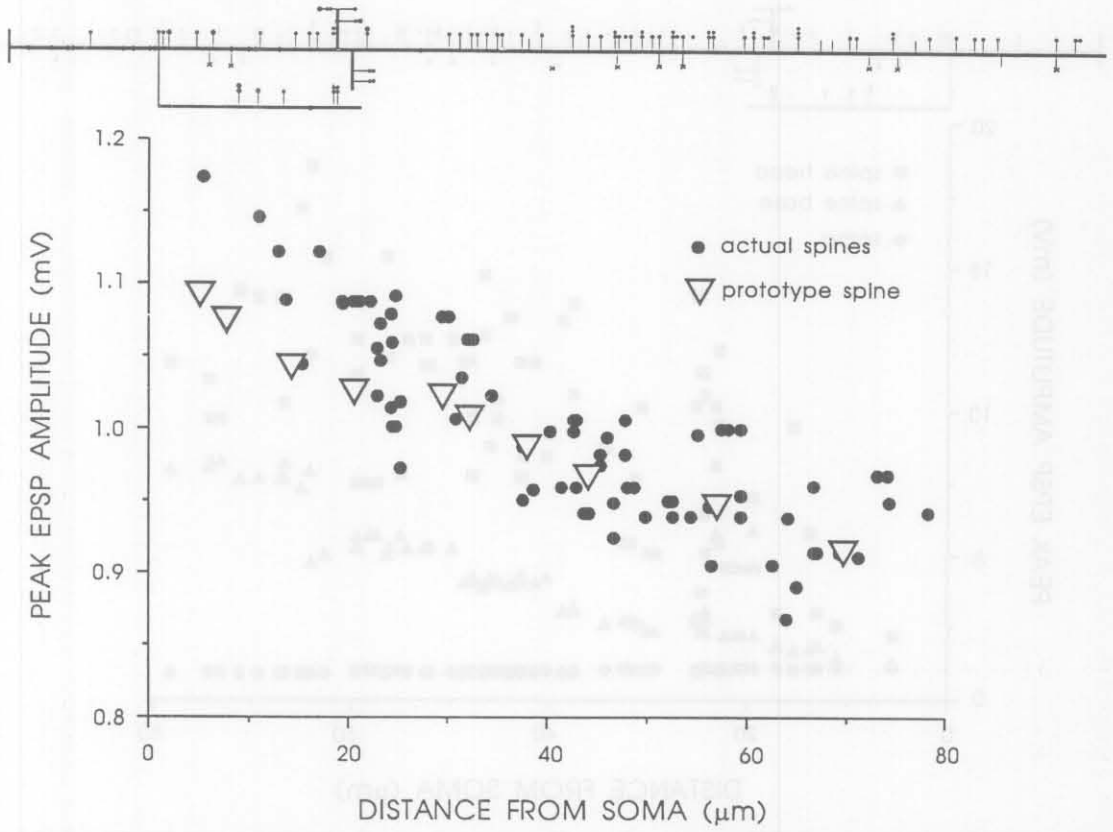

Figure 6. Amplitudes of unitary somatic EPSPs generated by the 75 asymmetrical axospinous synapses on dendrite 5 (inset), plotted as a function of distance from soma (filled circles). The amplitudes of the EPSPs range between 0.86 mV and 1.18 mV. Variability at a given distance mainly reflects the variability in spine neck lengths of all spines at this distance. Triangles show the expected EPSP that would result from activating the input on a prototype (average) spine (neck length = 0.9 μm, head diameter = 0.45 μm).

of TC synapses onto dendrites 1, 2, 3, 4, and 5 were 13, 7, 7, 6, and 10, respectively. The superimposed traces in Figure 8 show the composite somatic EPSP that results from simultaneously activating all 43 TC synapses on this cell (short dashed curve), and the EPSPs generated of separately activating the TC input to each of the dendrites (five continuous curves). The curve with long dashed line shows the somatic EPSP that would have been recorded had the activity from all the dendrites summed linearly. The TC input produced a rather powerful (30 mV) composite EPSP, which should be sufficient to achieve threshold for firing at the axon hillock (Agmon and Connors, 1992). The finding that summation of the synchronous TC input is not linear (15% less than linear) implies that the dendrites and spines are undergoing considerable depolarization while this input is active. This is to be expected for this neuron, which is so electrically small and has such a high input resistance. Indeed, for this distributed input, the whole tree undergoes approximately 30 mV peak depolarization.

As noted above, for individual spiny synapses that operate in a nonlinear range (close to saturation), changes in spine neck dimensions can have a significant influence on the amount of current generated (Rall, 1974; Rinzel, 1982; Koch and Poggio, 1983; Wilson, 1984). Figure 8 shows that with synchronous activation of all TC inputs, depolarization of the synapses reaches the nonlinear range. What would be the effect of changes in spine neck dimensions under these conditions, when many spines are activated at once? Theoretically, it can be shown that as the number of spines that undergo such a simultaneous change increases, the relative effect of this change becomes smaller, both

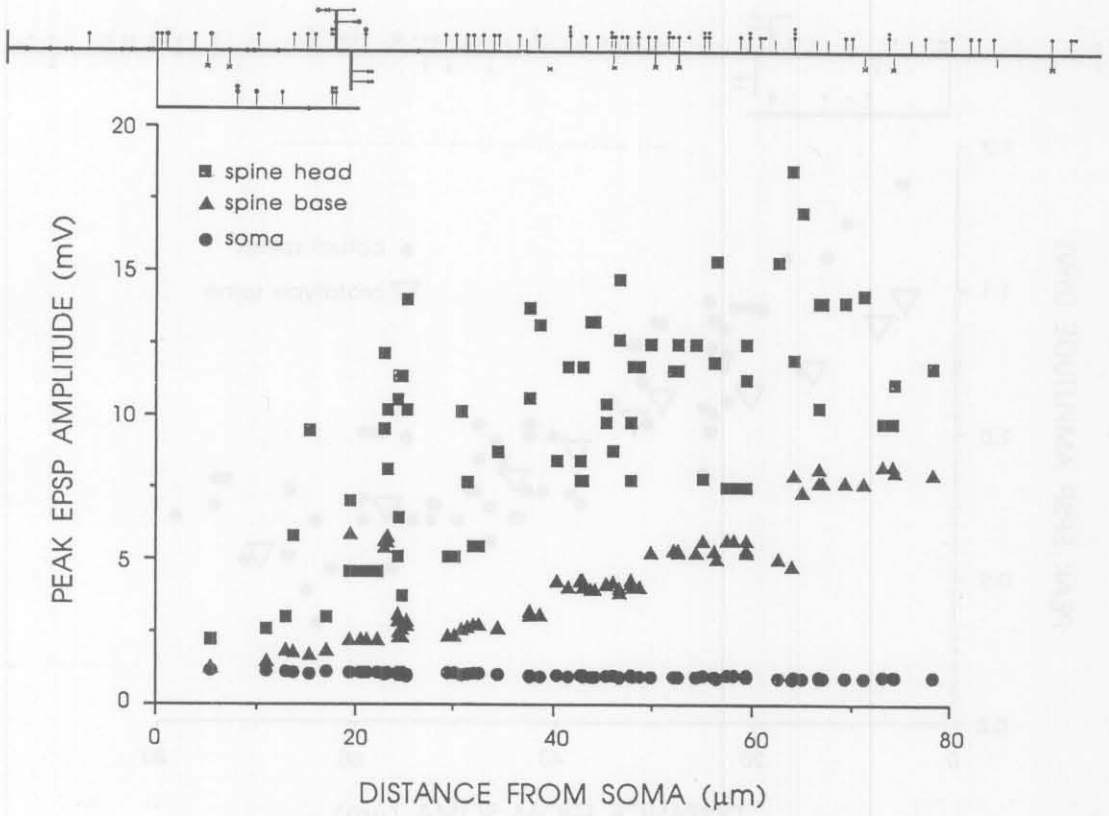

Figure 7. Amplitudes of unitary somatic EPSPs generated by the 75 asymmetrical axospinous synapses on dendrite 5 (inset), plotted as a function of distance from soma. Filled squares: at the spine heads. Filled triangles: at the spine bases. Filled circles: at the soma. Note that EPSP amplitudes vary by a factor of 10 at the spine heads and 5 at the spine bases; when viewed at this scale, there is essentially no variability in amplitudes of somatic EPSPs.

in the soma and in the dendrites (Segev, unpublished calculations). Indeed, this was verified here by changing the neck diameter of all 43 spines receiving TC input. As can be seen in Figure 9, when the diameters of the necks of the 43 spines were doubled to 0.2 μm, thereby decreasing all the R_{neck} values by a factor of 4, the resultant EPSP (dashed curve) was only minimally increased in amplitude (7%). When the 43 neck diameters were all halved to 0.05 μm, resulting in a fourfold increase in all R_{neck} values, the consequent decrease in the amplitude of the composite EPSP (dotted curve) was somewhat greater but still not particularly striking (12.8%). We conclude that with the parameters chosen, changes in spine neck morphology will not have a very significant effect on the depolarization produced by the TC input to this cell. Of course, changes in spine neck diameter of this magnitude would have a more significant influence on the cell's output if unitary synaptic conductance was greater or longer lasting.

Discussion

The detailed morphological information provided by the electron microscopic study of White and Rock 1980) has provided us with a unique opportunity to ask specific questions regarding the input-output function of cortical spiny stellate neurons. While several recent studies have demonstrated that neocortical dendrites do possess active conductances (Amitai et al., 1993; Kim and Connors, 1993; Regehr et al., 1993; Reuveni et al., 1993; Stuart and Sakmann, 1994; Markram and Sakmann, 1994), these have all focused on the apical dendrite of the cortical pyramidal cell. Because data regarding the electrical properties of the dendrites and dendritic spines of spiny stellate cells are not available, we have limited ourselves to exploring the passive case. With reasonable parameters for the electrical properties of the membrane and cytoplasm, and for the properties of the excitatory

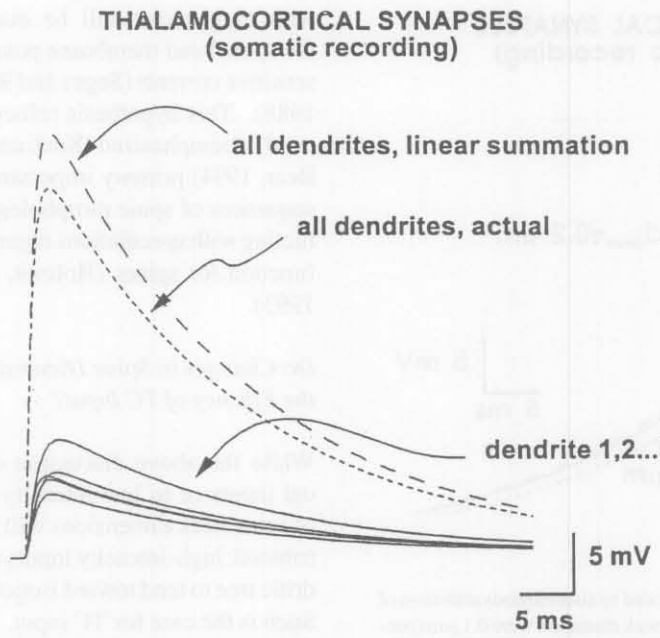

Figure 8. Somatic recordings of composite EPSPs generated (1) by simultaneous activation of TC synapses on each of the dendrites separately (five continuous curves) and (2) by synchronous activation of all 43 TC synapses (short dashed line). Long dashed curve shows the EPSP that would have been obtained had all five continuous curves summated linearly.

input, we could arrive at several general and robust conclusions.

How "Compact" Is This Electrically Compact Neuron?

From the soma viewpoint, the spiny stellate cell is electrically very short (0.2λ) for the representative R_m and R_i values chosen. Other central neurons—such as cerebellar Purkinje cells (Rapp et al., 1994), pyramidal cortical cells (Stratford et al., 1989), α-motoneurons (Fleshman et al., 1988)—were also estimated to be electrically "compact" (0.2 to 1.6λ). These values apply, of course, only to the steady-state condition. Moreover, compactness in this sense is a somato-centric concept. The implication is that, for compact cells, a significant portion of the synaptic current will reach the soma from the dendritic input site (Rall and Rinzel, 1973; Rinzel and Rall, 1974). This does not imply, however, that there is no voltage attenuation along the tree. As demonstrated in this study, even a very "compact" and morphologically simple tree exhibits a marked voltage gradient from individual input sites (spines) to the soma. What seems to be nearly isopotential from the somatic perspective is far from isopotential when viewed at points along the dendrite.

What Could Be the Functional Consequence of the Variability in the Spine Neck Length?

Complete reconstruction of a neuron using thin sections allows us to examine the dimensions of the whole spine population in this cell. The most striking finding is the enormous range of spine neck lengths, from very short necks of approximately 0.1 μm (mainly near the soma) to rather long spines (2 μm and more). Does this variability reflect some plastic processes that these spines (and their synapses) underwent, or is it a reflection of some morphological constraints (for example, going back to the old notion that "spines are to connect"; see Swindale, 1981)?

Our modeling study shows that were all the spines to receive identical glutaminergic (AMPA) inputs, the large variation in spine neck length would explain only 10% of the variability in the simulated somatic EPSPs; most of the variability in the simulated somatic EPSP amplitudes reflects the electronic structure of the neuron. This means that, under the assumptions of the present model, dendritic spines essentially operate as linear current sources with only a minor effect of synaptic nonlinearity at spine head membrane (Turner, 1984; Harris and Stevens, 1989). Combined with the small electrical dimensions of the cell, the EPSPs at

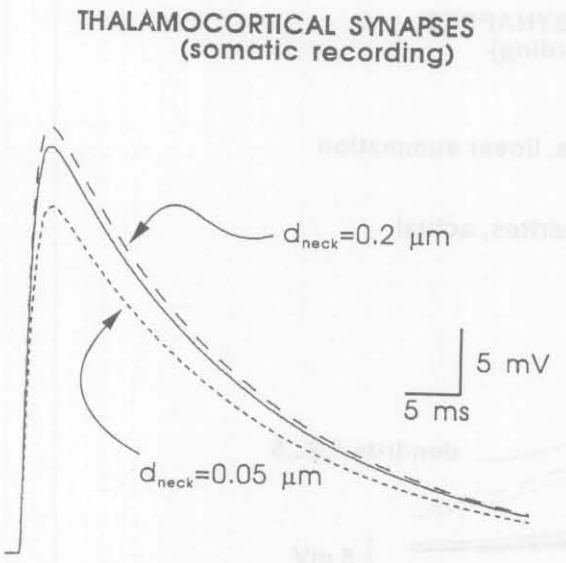

Figure 9. Composite EPSP generated by simultaneous activation of all 43 TC synapses when all spine neck diameters were 0.1 μm (continuous curve) and when all diameters were doubled (long dashed line) or were halved (short dashed curve). Note that the peak amplitude of the composite EPSP was relatively insensitive to changes in spine geometry.

the soma are essentially iso-efficient, regardless of the input site.

The variability in spine dimensions does, however, result in large differences in the EPSPs recorded locally at the spine head membrane. Single excitatory inputs onto spines with long necks produce significant (20 mV) depolarizations, whereas the postsynaptic membrane depolarizes by only a few mV in spines with short necks. If nonlinear channels (such as those activated by NMDA receptors or directly gated by voltage) are present on spines, they will be more easily activated on those with long necks (Segev and Rall, 1988). This raises the speculation that spines with long necks are sites where local plastic processes (e.g., activation of second messengers due to increased Ca^{+2} concentration at the spine head) were in progress at the time of brain fixation. This would suggest that spine neck dimensions do have important *electrical* consequences for local processing at the synapse, even though they have relatively little impact on the magnitude of the soma depolarization. By restricting local boosting of the synaptic input to those spines that have long necks (large R_{neck}), spine neck dimensions would preferentially facilitate activity-dependent plastic changes in only one subclass of the spine population. This selective boosting of potential in spines with long necks will be even more pronounced if the spine head membrane possesses excitable voltage-sensitive currents (Segev and Rall, 1988; Hillman et al., 1988). This hypothesis refocuses attention on the recently deemphasized (Koch and Zador, 1993; Gold and Bear, 1994) primary importance of the electrical consequences of spine morphology, while in no way conflicting with speculations regarding a possible chemical function for spines (Holmes, 1990; Koch and Zador, 1993).

Do Changes in Spine Dimension Directly Influence the Efficacy of TC Input?

While the above discussion does pertain to individual inputs or to low-intensity inputs, the significance of spine neck dimensions will diminish for widely distributed, high-intensity inputs that cause the entire dendritic tree to tend toward isopotentially (Wilson, 1992). Such is the case for TC input. Monosynaptic TC input to layer IV stellate cells in the mouse barrel cortex has been shown to be intense, of short latency, and mediated by non-NMDA receptors (Agmon and Connors, 1992; Agmon and O'Dowd, 1992; Armstrong-James et al., 1993). The EM study showed that approximately 10% of the excitatory synapses are innervated by TC axons and that these are evenly distributed throughout the dendritic tree. These values are in general agreement with more recent studies from spiny stellate cells in cat visual cortex (Ahmed et al., 1994), suggesting that they may reflect general features of the afferent innervation of this pivotal neuron in the thalamocortical path. The results illustrated in Figure 9 indicate that for such a distributed synchronous input, the relative sensitivity of the input/output function to changes in spine neck dimension would be even smaller than for single EPSPs. This is because with a distributed input, as significant depolarization develops in the entire dendritic membrane—spine and nonspine alike, the voltage gradients between spine heads and bases decrease, and changes in R_{neck} become accordingly less significant. The effect is particularly marked in a very compact neuron such as this, since the individual synaptic membranes are driven well into the nonlinear range, as shown in Figure 8.

Previous speculations on the functional significance of a spine's dimensions have focused on possible direct, electronic consequences on synaptic efficacy, as measured at the soma in simple input/output terms. However, our simulations lead us to conclude, as have others (Turner, 1984; Kawato and Tukahara, 1984;

Harris and Stevens, 1989; Koch and Zador, 1993), that it is unlikely that the primary role of the spine is to modulate the amplitudes and hence the effectiveness of somatic potentials in this way. This does not mean that spine dimensions have no electrical consequences. On the contrary, once our focus shifts from a somato-centric to a dendro-centric perspective, we perceive that in the dendrites, changes in spine dimensions have a direct and significant electrical effect. It is likely that processes such as LTP and LTD, which may be extremely significant determinants of input to the cell, are triggered by local voltage changes in spines. As our simulations illustrate, the voltage changes induced by changes in spine dimensions can be profound enough locally near the synapses to significantly modulate such processes, while having only minimal influence on spike firing from the soma.

Acknowledgments

We thank Orit Loifer for help implementing the model in SPICE and Dahlia Weizmann for preparing the dendrogram in Figure 3. This study was supported by grants from the Deutsche Forschungsgemeinschaft (SFB 194/B3) to MJG, the Office of Naval Research to IS, and the Israel Academy of Sciences and Humanities (618/93) to ELW.

References

Agmon A and Connors BW (1992) Correlation between intrinsic firing patterns and thalamocortical synaptic responses of neurons in mouse barrel cortex. *J. Neurosci.* 12:319–329.

Agmon A and O'Dowd DK (1992) NMDA receptor-mediated currents are prominent in the thalamocortical synaptic response before maturation of inhibition. *J. Neurophysiol.* 68:345–349.

Ahmed B, Anderson JC, Douglas RJ, Martin KAC, and Nelson JC (1994) Polyneuronal innervation of spiny stellate neurons in cat visual cortex. *J. Comp. Neurology* 341:39–49.

Amitai Y, Friedman A, Connors BW, and Gutnick MJ (1993) Regenerative activity in apical dendrites of pyramidal cells in neocortex. *Cerebral Cortex* 3:26–38.

Armstrong-James M, Welker E, and Callahan CA (1993) The contribution of NMDA and non-NMDA receptors to fast and slow transmission of sensory information in the rat SI barrel cortex. *J. Neurosci.* 13:2149–2160.

Benshalom G (1989) Structural alterations of dendritic spines induced by neural degeneration of their presynaptic afferents. *Synapse* 4:210–222.

Brown TH, Chang VC, Ganong AH, Keenan CL, and Kelso SR (1988) Biophysical properties of dendrites and spines that may control the induction and expression of long-term synaptic potentiation. In: PW Landfield and SA Deadwyler, eds. Long-Term Potentiation: From Biophysics to Behavior. Alan R. Liss New York, NY. pp. 201–264.

Crick F (1982) Do dendritic spines twitch? *Trends in Neurosci.* 5:44–46.

Fleshman JW, Segev I, and Burke RE (1988) Electrotonic architecture of type-identified α-motoneurons in the cat spinal cord. *J. Neurophysiol.* 60:60–85.

Gold JI and Bear MF (1994) A model of dendritic spine Ca^{+2} concentration exploring possible basis for a sliding synaptic modification rule. *Proc. Nat. Acad. Sci.* 91:3941–3946.

Harris KM and Stevens JK (1989) Dendritic spines of CA1 pyramidal cells in the rat hippocampus: serial electron microscopy with reference to their biophysical characteristics. *J. Neurosci.* 9:2982–2997.

Hillman D, Chen S, Aung TT, Cherksey B, Sugimori M, and Llinas R (1991) Localization of P-type calcium channels in the central nervous system. *Proc. Nat. Acad. Sci.* 88:7076–7080.

Hines M (1989) A program for simulation of nerve equations with branching geometries. *Int. J. Biomed., Comput.* 24:55–68.

Holmes WR (1990) Is the function of dendritic spines to concentrate calcium? *Brain Research* 519:338–342.

Kawato M and Tsukahara N (1984) Electrical properties of dendritic spines with bulbous end terminals. *Biophys. J.* 46:155–166.

Kim HG and Connors BW (1993) Apical dendrites of the neocortex: correlation between sodium- and calcium-dependent spiking and pyramidal cell morphology. *J. Neurosci.* 13:5301–5311.

Koch C and Poggio T (1983) A theoretical analysis of electrical properties of spines. *Proc. R. Soc. Lond.* 218:455–477.

Koch C and Zador A (1993) The function of dendritic spines: Devices subserving biochemical rather than electrical compartmentalization. *J. Neurosci.* 13(2):413–422.

Markram H and Sakmann B (1994) Calcium transients in dendrites of neocortical neurons evoked by single subthreshold excitatory postsynaptic potentials via low-voltage-activated calcium channels. *Proc. Nat. Acad. Sci.* 91:5207–5211.

Nitzan R, Segev I, and Yarom, Y (1990) Voltage behaviour along the irregular dendritic structure of morphologically and physiologically characterized vagal motoneurons in the guinea pig. *J. Neurophys.* 63:333–346.

Rall W (1964) Theoretical significance of dendritic trees for neuronal input-output relations. In: R Reiss, ed. Neural Theory and Modeling. Stanford U. Press, Stanford, CA. pp. 73–97.

Rall W (1967) Distinguishing theoretical synaptic potentials computed for different soma-dendritic distributions of synaptic input. *J. Neurophysiol.* 30:1138–1168.

Rall, W (1974) Dendritic spines, synaptic potency and neuronal plasticity. In: CD Woody, KA Brown, TJ Crow, and JD Knispel, eds. Mechanisms Subserving Changes in Neuronal Activity. Brain Information Service Research Report Vol. 3, Los Angeles, CA. pp. 13–21.

Rall W and Rinzel J (1973) Branch input resistance and steady attenuation for input to one branch of a dendritic neuron model. *Biophys. J.* 13:648–688.

Rapp M, Segev I, and Yarom Y (1994) Physiology, morphology and detailed passive models of cerebellar Purkinje cells. *J. Physiol.* (London) 474:101–119.

Regehr W, Kehoe JS, Ascher P, and Armstrong C (1993) Synaptically triggered action potentials in dendrites. *Neuron* 11:145–151.

Reuveni I, Friedman A, Amitai Y, and Gutnick MJ (1993) Stepwise repolarization from Ca^{2+} plateaus in neocortical pyramidal cells:

Evidence for nonhomogeneous distribution of HVA Ca^{2+} channels in dendrites. *J. Neurosci.* 13:4609–4621.

Rinzel J (1982) Neuronal plasticity (learning), *Lect. Math. Life Sci.* 15:7–25.

Rinzel J and Rall W (1974) Transient response in a dendritic neuron model for current injected at one branch. *Biophys. J.* 14:759–790.

Segev I, Fleshman JW, and Burke RE (1989) Compartmental models of complex neurons. In: C Koch and I Segev, eds. Methods in Neuronal Modeling: From Synapses to Networks. MIT Press, Boston, MA. pp. 63–96.

Segev I, Fleshman JW, Miller JP, and Bunow B (1985) Modeling the electrical behavior of anatomically complex neurons using a network analysis program: passive membrane. *Biol. Cybernetics* 53:27–40.

Segev I and Rall W (1988) Computational study of an excitable dendritic spine. *J. Neurophysiol.* 60:499–523.

Segev I, White EL, and Gutnick MJ (1989) Detailed compartmental model of an em reconstructed spiny stellate cell in the mouse neocortex. *Society for Neuroscience Abstracts* 15:256.

Stern P, Edwards FA, and Sakmann B (1992) Fast and slow components of unitary EPSCs on stellate cells elicited by focal stimulation in slices of rat visual cortex. *J. Physiol.* 449: 247–278.

Stratford AU, Mason A, Larkman AU, Major G, and Jack JJB (1989). The modeling of pyramidal neurons in the visual cortex. In: R Durbin, C Miall, and G Mitchison, eds. Addison Wesley, Worhengham, England. pp. 296–321.

Stuart GJ and Sakmann B (1994) Active propagation of somatic action potentials into neocortical pyramidal cell dendrites. *Nature* 367:69–72.

Swindale NV (1981) Dendritic spines only connect. *Trends in Neurosci.* 4:240–241.

Thomson AM and West DC (1993a) Fluctuations in pyramid-pyramid excitatory postsynaptic potentials modified by presynaptic firing pattern and postsynaptic membrane potential using paired intracellular recording in rat neocortex. *Neurosci.* 54: 329–346.

Thomson AM, Deuchars J, and West DC (1993b) Single axon excitatory post synaptic potentials in neocortical interneurons exhibit pronounced paired pulse facilitation. *Neurosci.* 54:347–360.

Turner DA (1984) Segmental cable evaluation of somatic transients in hippocampal neurons (CA1, CA3, and dentate). *Biophys. J.* 46:73–84.

White EL (1989) Cortical Circuits. Synaptic Organization of the Cerebral Cortex; Structure, Function and Theory. Birkhauser Press, Boston.

White EL and Rock MP (1980) Three-dimensional aspects and synaptic relationships of a Golgi-impregnated spiny stellate cell reconstructed from serial thin sections. *J. Neurocytol.* 9:615–636.

Wilson CJ (1984) Passive cable properties of dendritic spines and spiny neurons. *J. Neurosci.* 4:281–297.

Wilson CJ (1992) Dendritic morphology, inward rectification, and functional properties of neostriatal neurons. In: T McKenna, J Davis, and SF Zanetzer, eds. Single Neuron Computation. Academic Press, San Diego, CA. pp. 141–171.